MedLife Clinics

ISSN: 2689-5943

Research Article

Identified of Potential Therapeutic Targets for Salivary Gland Adenoid Cystic Carcinoma by Bioinformatic Analysis

Ailing Hu[1], Yuan Gu[2], Takuji Yamaguchi[1], Han Liu[3], Yuuko Uehara[1], MutsuhitoUi[1], Shigeko Okuno[1], Daisuke Watanabe[1], Shinobu Mizushima[1], Qijin Feng[2], Shilin Xia[1,4] and Akio Mizushima[1]**

[1]Department of Palliative Medicine, Graduate School of Medicine, Juntendo University, Tokyo, Japan

[2]Center for Advanced Kampo Medicine and Clinical Research, Graduate School of Medicine, Juntendo University, Tokyo, Japan

[3]Department of Oral Pathology, Dalian Medical University, Dalian, China

[4]Clinical Laboratory of Integrative Medicine, The First Affiliated Hospital of Dalian Medical University, Dalian, China

Abstract

Salivary Gland Adenoid Cystic Carcinoma (SACC) is the most common type of salivary gland malignancy associated with inferior chemoradiotherapy, which behaves unfavorable prognosis and poor overall survival. There is a growing body of literature that focuses on the biomarker research. However, only a limited number of pharmaceutical targets have been identified. The objectives of this research are to screen the potential biomarker from microarrays and determine the putative drug target by bioinformatics analysis. To identify hub genes, microarrays data was downloading from Gene Expression Omnibus (GEO) in order to screen 1282 genes. Functional analysis and pathway enrichment were addressed using DAVID. After 47 hub genes felted by STRING and Cytoscape, 18 candidates drug targets were performed using Oncomine analyses. The network of these potential biomarkers was provided with cBio Portal online analysis. In conclusion, this study offers some insights into understanding the link between the effective bioinformatics approach and potential biomarker, which makes a contribution to therapeutic targets research.

Keywords: Salivary gland adenoid cystic carcinoma; Differentially expressed genes; Microarray; Pharmaceutical target

Introduction

Adenoid Cystic Carcinoma (ACC), including salivary gland and some other organs, is rare type of malignant tumors [1,2]. Among ACC, Salivary Gland Adenoid Cystic Carcinoma (SACC) is one most common type even though the underlying mechanism of SACC is generally unknown. Evidence suggests that abnormal expression is among the most important factors for driving the occurrence and procession of carcinoma [3,4]. The profile of expression has recently been investigating by high throughput technology, such as genomics sequencing and expression profile microarray [5,6]. Therefore, it is indicated that the expression profile analysis of SACC from datasets of Gene Expression Omnibus (GEO) would contribute to effective therapeutic strategies. However, research to date has not yet determined enough variety of drug clues but only limited in number. The study need be carried out to find more scientific evidence to investigate the correlation between molecular mechanism and clinical therapy. It is therefore set out to assess available data and thus promote the development of SACC medicine.

During the decades, expression profile experiment is frequently prescribed for analysis of DEGs functional process. Microarrays have been widely used to detect the expression profile alterations. Microarray technology is fundamental to bioinformatic analysis. In this research, bioinformatic data was obtained from 2 mRNA microarray between normal human salivary gland tissue and SACC. The overlap of Differentially Expressed Genes (DEGs) was analyzed with Gene Oncology (GO) and Kyoto Encyclopedia of Genes and Genomes (KEGG). Subsequently, the most significant network of hub genes was determined using STRING online, which was visualized by Cytoscape plug in MCODE. The candidate genes selection was proposed with Oncomine analysis. The potential therapeutic targets were finally performed with cBio Portal online analysis. This study would provide new sights into foundation of SACC treatment strategy.

Materials and Methods

Raw data from microarray data

Expression profile of microarray was obtained from GEO [7]. GEO is a public gene expression data pool of high throughput sequencing and SAGE array, genome tilting array and SNP array. Based on the screening salivary gland adenoid cystic carcinoma datasets, there are 13 datasets with the parameter of Homo sapiens and Series. The 2 datasets of GSE88804 and GSE36820 were determined to analyze the different gene expression between normal human salivary glands and carcinoma samples. GSE88804 is the dataset from Sahlgrenska Cancer Center of University of Gothenburg [8]. GSE36820 is the dataset from Advanced Biomedical Computing Center of SAIC-Frederick.

Citation: Ailing Hu, Yuan Gu, Yamaguchi T, Liu H, Uehara Y, Mutsuhito Ui, et al. Identified of Potential Therapeutic Targets for Salivary Gland Adenoid Cystic Carcinoma by Bioinformatic Analysis. Med Life Clin. 2019; 1(1): 1005.

Publisher Name: Medtext Publications LLC

Manuscript compiled: October 10th, 2019

***Corresponding author:** Akio Mizushima, Department of Palliative Medicine, Graduate School of Medicine, Juntendo University, Tokyo, Japan, E-mail: akiom@juntendo.ac.jp

Shilin Xia, Department of Palliative Medicine, Graduate School of Medicine, Juntendo University, Tokyo, Japan, E-mail: shilin320@126.com

Identification of SACCDEGs

GEO2R were applied to screen the DEGs between normal human salivary glands and carcinoma samples. GEO2R is a web tool to compare groups in the dataset in order that researchers can obtain the differentially expressed genes. The absolute value of fold change ≥ 1.5 and adj. P value ≤ 0.01 were considered statistically significant. The overlap result of DEGs was constructed using Venn diagram online analysis, which was recorded by graphical output.

GO and KEGG analysis of DEGs

The biological process and signal pathway information was carried out using DAVID (version 6.8) [9]. DAVID is a bioinformatics resource of functional annotation and gene functional classification. After entering gene list and selecting identifier and species, the functional annotation chart of GO was displayed including Biological Process (BP), Cell Component (CC) and Molecular Function (MF). GO analysis is an online tool to annotate the selected genes [10]. The pathway analysis of DEGs was performed using KEGG analysis. KEGG is a database of signal pathway to understand the systemic pipelines of molecular, which was generated by experimental technologies [11]. P value ≤ 0.05was considered statistically significant.

Network construction of DEGs

The STRING (version 11.0) was applied to construct the interaction network of proteins [12]. The STRING is a web tool to generate the functional interaction of molecular, which provides the insights of the interaction and mechanism of DEGs. The score= 0.900 was considered statistically significant. According to the data obtained from STRING, protein-protein interaction of DEGs was generated using Cytoscape (version 3.7.1) with plug-in MCODE (Molecular Complex Detection). MCODE is a Cytoscape app that finds clusters (highly interconnected regions) in a network [13]. The MCODE (version 1.5.1) used presented here was designed by Bader Lab in University of Toronto. The configuration of MCODE was as follows: Node score Cutoff=0.2, K-Core=2, Degree Cutoff=2, Max. Depth=100.

Analysis of hub gene

We made a concrete analysis of hub genes in salivary gland adenoid cystic carcinoma on the platform of Oncomine. The datasets of Oncomine are composed of samples represented as microarray data [14]. The Frieerson HF salivary-gland dataset is only one dataset of SACC in the platform [15]. After selecting the filter of analysis type and cancer type, we investigated each of hub gene in order that candidate genes were evaluated between normal and cancer type. Analysis Type: Cancer *vs.* Normal Analysis, Cancer Type: Salivary Gland Adenoid Cystic Carcinoma.

Pharmaceutical target analysis of candidate gene

The network and pharmaceutical target analysis of candidate genes were performed using cBio Portal [16]. The cBio Portal is an online tool for analyzing cancer genomics information and biological interaction network. The use of cBio Portal is a well-established approach to perform and visualize pharmaceutical target of candidate gene. The adenoid cystic carcinoma constructed in 2015 contains a total of 102 samples, which is the most data module in Head and Neck Query. Filter Neighbors by Alteration was set 10%. The drug included FDA approved drugs and Not-FDA approved drugs.

Results

Identification of DEGs in ACC

For the purpose of analysis, two SACC datasets were extracted from GEO database. GSE88804 and GSE36820 were identified. The total of differentially expressed genes was 11552 in GSE88804 and 4427 in GSE36820 respectively. The overlap genes contained a total of 1282 DEGs, which was exhibited in the Venn diagram (Figure 1A).

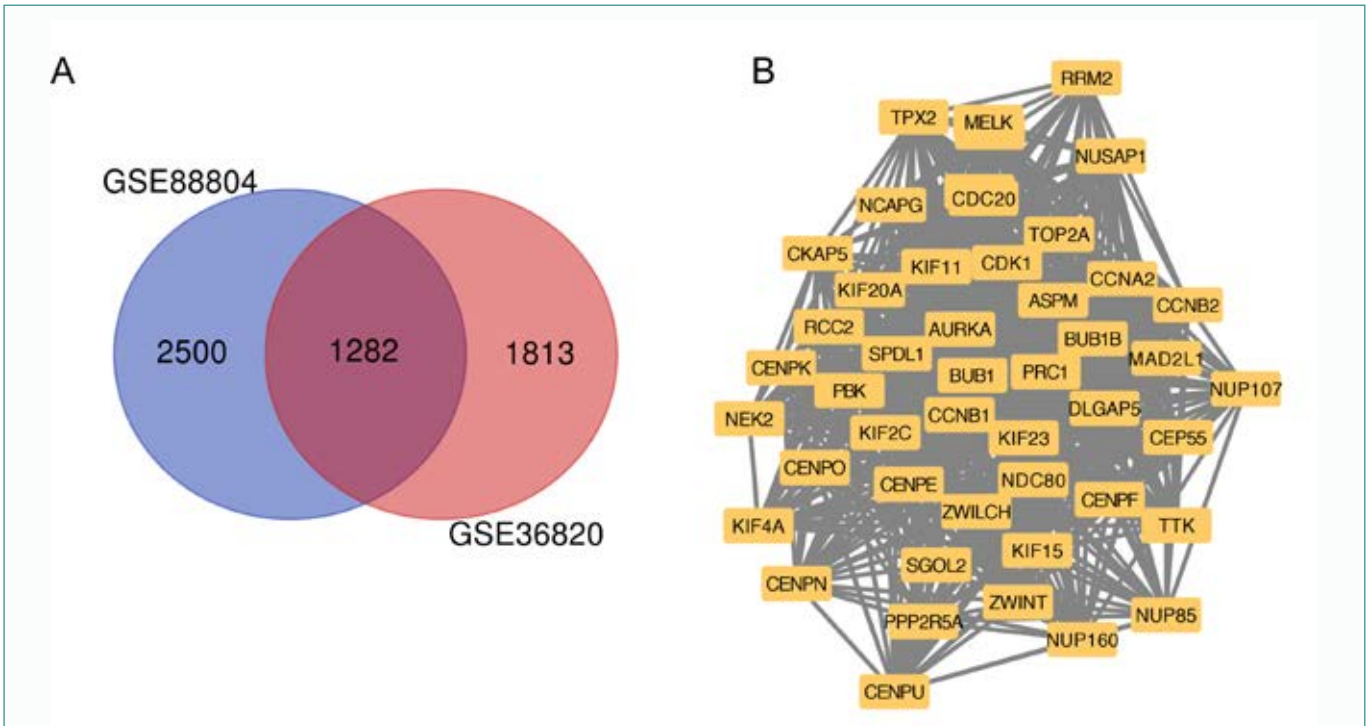

Figure 1: Venn diagram and the most significant module of DEGs. (A) DEGs were selected with the absolute value of fold change ≥ 1.5 and adj. P value ≤ 0.01 among the mRNA expression profiling datasets GSE88804 and GSE36820. These 2 datasets showed an overlap of 1282DEGs. (B) The most significant module was obtained from Cytoscape plugin MCODE.

Table 1: GO analysis of DEGs in SACC samples.

Term(BP, CC,MF)	Count	%	PValue	Genes
BP:GO:0007165~signal transduction	94	7.5019952	0.0423975	MOK, NAMPT, GNA14, ACVRL1, SLC44A2, PPP2R5A, IL19, IQGAP3, TNFSF15, PDE3B, IQGAP2, TLR3, FGF12, PRKG1, CXCL12, KCNIP3, PGR, TNFRSF11A, LILRA2, ANK2, PDE4A, GATA3, PDE4B, IL15RA, IL1B, PDE8B, PITPNC1, UNC5C, PRKACB, PAG1, KHDRBS1, RSU1, MPP1, NRXN3, PLXNB1, PRKCH, TNFRSF17, DEPDC1, NRXN1, OPTN, ARHGAP24, ARHGAP26, DAPK1, VEGFC, NPC1, RIN2, PDE9A, STMN1, RASD1, SRGAP1, KALRN, PLPP5, ERBB4, RAP1GAP, GULP1, C3, PPP4R1, NR3C2, CCL8, NOSTRIN, NR3C1, CXXC5, APBB1IP, FAM13A, STARD13, RGS12, DAPP1, BCL11A, AGRN, INPP5D, NDRG2, EGF, PLA2R1, CDC42EP3, GABRP, NKRF, C1ORF168, NR4A2, NDFIP1, ANXA1, COL15A1, IGF1, SPARC, RACGAP1, STAT3, APOL3, PDE7B, TNFSF10, PLCG1, CD274, RAP1A, ADRA1A, WIF1, IGFBP2
BP:GO:0051301~cell division	63	5.027933	1.66E-12	CDK19, MAEA, AURKA, PTTG1, FAM83D, KIF2C, CDCA7, CCNA2, CDCA4, KIF14, CDC7, CDK1, CDC6, ARHGEF2, KIF11, TPX2, PAPD7, CDK6, MCM5, WEE1, NCAPD2, MAD2L1, RCC2, GO2, TIMELESS, ZWINT, BUB1B, UBE2S, CKS1B, NEK2, HAUS1, LRRCC1, NR3C1, CNTRL, CCNG2, VRK1, TUBB, NCAPH, NCAPG2, FIGN, NCAPG, BUB1, SKA3, FBXO5, ZWILCH, HELLS, CKAP5, NUF2, CENPF, NDC80, CENPE, CDC20, SPDL1, CDC25C, SMC2, CENPJ, SMC4, CDC25B, CCNB1, CCNB2, KNL1, CKS2, PARD6G
BP:GO:0000122~negative regulation of transcription from RNA polymerase II promoter	62	4.9481245	0.037205	CPEB3, E2F7, EZH2, WWC1, PAWR, ZKSCAN3, GATA3, HEY2, H2AFY, ZFP36, SATB1, SP100, CTBP2, ZNF280C, TP53, LEF1, ZNF8, JUNB, ASCL2, HES1, TRIM37, UHRF1, CD36, TIMELESS, SIX1, TFAP2B, TFAP2A, ZNF431, TGIF2, SMARCA4, FGFR1, TSHZ2, FOXM1, ZBTB16, CXXC5, TCF7L2, TSC22D3, MEIS2, XBP1, SQSTM1, NRARP, BCL11A, CHD4, RFX5, TRIM28, ASXL1, NR4A2, EN1, SMAD2, STAT3, FOXP2, FNIP2, NOTCH3, NOTCH1, HDAC2, TRPS1, H2AFY2,HOPX, DNMT1, HDAC9, TBL1X, CRYM
CC:GO:0005737~cytoplasm	427	34.078212	3.85E-08	PTGS2, PPP2R5A, SART3, ACBD6, B2M, WDR72, APP, CDCA7, RAE1, CCNA2, SYK, UBE2J1, SKP2, NAA25, NCAPD2, ZWINT, ODAM, KIF4A, DNAH14, GSTCD, UBA5, CNTRL, TPGS2, CASZ1, CDC42EP3, MKI67, JTB, FNIP2, APOL3, RGS2, PCNA, SYTL4, SLC9A1, SEPHS1, EZH2, HSF2, WDR35, CDC7, SH3PXD2B, CDC6, ARHGEF2, PAPD7, TP53, CCT6A, ARHGEF9, FLNA, TTF2, MAST4, FANCD2, CKAP2L, RRM2, CLIC6, RRM1, SERPINB1, TXK, CAND1, THOC5, ARL4D, SRGAP1, ARL4A, REPS2, ALDH18A1, ABHD5, EPB41L4A, ABI2, EPB41L4B, FMO5, MT1E, BUB1, MT1F, FLRT3, ZNF260, DGKH, MID1, CABYR, CCNB1, MPHOSPH9, RASSF5, DUSP1, AOX1, MT2A, DPYD, PHLDB2, BARD1, DUSP6, TSPAN1, GNPDA1, PRC1, XPO5, STK36, IQGAP2, SLC7A5, IL17RB, LNX1, EIF4EBP1, ASPA, ATAT1, MDFIC, C8ORF4, RGN, PITPNC1, STK39, DNAJC3, ASPM, RBFOX2, ACTN4, STK26, FBP1, ACTN1, CHODL, TMSB10, WEE1, DDIT4, ASCL2, HSPB8, IX1, TFAP2A, STMN1, NEU3, LRRK2, SLC40A1, CRACR2A, CCDC8, HMGB2, HMGB3, LRRCC1, CXXC5, CCNG2, PRUNE2, OAZ3, ISYNA1, TUBB, GINS1, NR4A2, BRIP1, EFS, FAM208B, WIPI1, DNAJB9, HDAC2, FABP4, PMP2, FABP7, HDAC9, MYH10, KIF22, E2F3, FIGNL1, WWC1, GABBR1, PAWR, ZKSCAN3, SH2D4A, PRMT3, PRMT1, CDC45, SPRY1, LBH, TRIM8, HEY2, NTB1, KDM5B, CASP2, CDK1, METTL8, ZCCHC2, KIF11, LIMK2, NUSAP1, CDK6, SRPRB, MAN1A1, DHRS2, RFWD3, TBCB, ATG4A, FRMD4A, ERN1, HORMAD1, CA2, SPATS2L, STON2, PLPP5, ABLIM1, HYLS1, VIM, HAUS1, TYW5, NR3C1, NDC1, TSC22D1, ALDH1A1, ADIRF, TSC22D3, WDPCP, INPP5J, FIGN, PAFAH1B3, CHD4, EXO1, RNF144B, ADARB1, GMDS, BBOF1, MZB1, ANXA1, EXO5, SMC2, RCAN2, CDC25B, SMC4, CCDC110, ITPA, ZBED4, SH3BGRL2, DSC3, KDM4A, DMBT1, CTTNBP2NL, MOK, PRR11, PTTG1, LPAR1, PRKG1, AQP3, ATP2B2, G2E3, CD44, TRAK2, RBM8A, HOMER3, POLH, BYSL, WNK3, OPTN, NUDT11, CD40, VASH2, FARP2, HES1, DCLRE1B, PIAS3, CCR2, RGCC, CNTROB, DBN1, FBXL2, NEK2, AKAP12, MME, TIPRL, VRK1, FBXO5, SKA3, AGRN, WDHD1, OLFM2, HNRNPAB, SRP54, BHMT2, UAP1, SMAD9, SMYD3, CIDEA, EPRS, CDC20, CELSR2, TPD52L1, SMAD2, CEP85L, HOMER2, NOTCH3, NTRK3, CCT5, HOPX, RAD54B, CRYM, CPEB3, CPEB4, TTLL4, TTLL7, TTLL1, FANCI, FAM129A, TOP2A, ZFP36, CEP112, NIP7, POLR1B, RAD51, TESMIN, FARSB, RIN2, FUT8, GULP1, BDP1, CLDN10, SEC14L1, XBP1, SQSTM1, NCAPG, PLIN4, BCL2, BCL11A, SULT1C2, KIF21A, AFAP1, FAM89B, NOS1, DLGAP5, ILF3, BIRC3, CDKN3, STAT3, C4ORF46, MEOX2, CHML, NUPR1, KNL1, MEX3C, APBB2, BAMBI, PAICS, TEX10, CALM1, ALDH1L1, MAEA, TTK, DSTYK, TLR3, ALDH1L2, MCM10, PNP, KLHL2, KLHL7, NANS, TRIM45, SPR, MLKL, RNF34, DDX39A, CEP89, DTL, BASP1, ME TTL7A, ELL2, TRIM37, TNS1, SDCBP, SNRPA, DSP, RIPK4, ERC1, EIF4E3, PODN, BLM, GNE, SOX4, GIPC2, RRAGD, CMPK1, NDRG2, MFAP3L, GNMT, DDIAS, CKAP2, SETDB1, TESC, LPO, EEF1A2, RPGRIP1L, RIMKLB, PLCG1, GLMN, RAP1A, TMPO, FAM84B, NAMPT, CEP57L1, NCS1, PDCD4, BZW2, FAM83D, MCM7, PAK3, SDPR, CAMSAP1, ACOT11, PARM1, SP100, CCDC88C, RUNX1T1, PRKCH, LEF1, MCM2, ARHGAP29, ECT2, RTTN, DAPK1, CTH, SMTN, BUB1B, NRK, KIAA0513, UBE2S, KPNA2, UBE2T, SPAST, AOC3, SHCBP1, FOXM1, KIAA0101, CYTH2, PALMD, TCF7L2, TYMS, RGS12, HJURP, APEX1, MSH6, GLRB, CENPF, CENPE, SPARC, RACGAP1, SLC17A5, TDP1

CC:GO:0005634~nucleus	386	30.806065	0.0290561	PTGS2, PPP2R5A, RORC, SART3, PGR, CDCA7, RAE1, WDR76, PHTF2, CCNA2, CDCA4, SYK, VWA5A, ZNF506, SKP2, NCAPD2, RCC2, ZWINT, ZNF239, TGIF2, VGLL4, ZNF614, ODAM, ERBB4, ZNF77, UBA5, ZNF230, ZNF618, PUS7, NCAPG2, PIP, CASZ1, NAT10, ZNF529, MKI67, GGH, NUF2, ESRRG, NDC80, SPDL1, KLF15, ACPP, RGS2, PKP2, TRPS1, PCNA, HLF, EZH2, NAP1L3, ZNF678, ZNF738, ZNF682, HSF2, ZNF681, ZNF492, CDC7, NFKBIZ, CDC6, EXOSC7, PAPD7, TPX2, TP53, HN1, FLNA, FANCD2, ZNF135, RRM2, CLIC6, CAND1, TXK, THOC5, RASD1, ARL4A, ZNF558, ZNF556, ABHD5, SF3B3, ZNF850, MT1E, TBC1D1, MT1F, TRIP13, TRIM28, ZFP1, ZNF667, DGKH, CABYR, CCNB1, ZNF670, RASSF5, CCNB2, DUSP1, MT2A, ZBTB5, USP49, BARD1, PRC1, XPO5, STK36, SNRPD1, ASPA, BHLHA15, MDFIC, ZNF300, C8ORF4, RGN, DDX21, STK39, ASPM, DNAJC1, MTUS1, RBFOX2, ACTN4, STK26, ZNF8, MND1, ZNF3, WEE1, ASCL2, FP69B, SMARCE1, TIMELESS, HSPB8, SIX1, TFAP2B, TFAP2A, ZNF431, CRACR2A, SMARCA4, HMGB2, HMGB3, NOSTRIN, IL33, MEIS1, ZNF330, OAZ3, TUBB, MEIS2, HELLS, GINS1, GINS2, NR4A2, BRIP1, TEAD2, FAM208B, IDH3A, HDAC2, FABP4, ADRA1A, HDAC9, DDX52, MYH10, ZKSCAN7, KIF23, KIF22, E2F3, FIGNL1, E2F7, WWC1, CAD, PAWR, ZKSCAN3, KIF2C, PRMT1, CDC45, LBH, PAX9, HEY2, KDM5B, CASP2, KIF14, METTL8, CDK1, ZNF280C, LIMK2, NUSAP1, CDK6, DIEXF, PBK, DHRS2, ADRB2, RFWD3, HORMAD1, HYLS1, NR3C2, NFYB, NR3C1, NFYA, TSPYL4, TSPYL5, APLP2, TSC22D1, ADIRF, TFAM, TSC22D3, FIGN, HMGXB3, CHD4, EXO1, PDCD11, ADARB1, KLK3, CEBPD, CEBPG, ANXA1, KLK1, EXO5, CDC25C, SMC2, FBL, SMC4, CCDC110, ZBED4, KDM4A, TBL1X, MOK, ALAD, S100A8, PRR11, AURKA, PTTG1, AQP3, TRAK2, RBM8A, H2AFY, CREB3L1, PRAME, BYSL, OPTN, DEPDC1, NUDT11, HES1, ZFP82, UHRF1, MAD2L1, RGCC, FUS, NEK2, STK17B, CHEK1, VRK1, FBXO5, OLFM2, MOCS1, HNRNPAB, PLAG1, NKRF, SRP54, KLF7, SMAD9, CIDEA, SMAD2, EN1, CDC20, HOMER2, ABCG2, ZFHX4, NOTCH1, NOP16, CSRNP1, HOPX, RAD54B, CRYM, RPP40, ATAD2B, CPEB3, CPEB4, SOBP, ZBTB38, KCNIP3, RBM47, TOP2A, ZFP36, CTBP2, NIP7, POLR1B, ZFP37, RAD51, TESMIN, YPEL1, LCORL, ZBTB16, NCAPH, XBP1, NCAPG, FAT1, BCL2, BCL11A, ETV1, DLGAP5, ILF3, BIRC3, CDKN3, STAT3, NUPR1, MEOX2, KNL1, MEX3C, APBB2, CALM1, MAEA, FGF10, CBX3, FGF12, CBX1, MCM10, PNP, KLHL7, TIAM1, GATA3, RNF34, RPL36AL, DDX39A, ARGLU1, SATB1, C2CD2, DTL, BASP1, SDCBP, DSP, AKAP7, CPD, FGFR1, TSHZ2, BLM, MSMB, DIAPH3, SOX4, RRAGD, CMPK1, MFAP3L, DDIAS, SETDB1, CSTF3, TESC, RFX5, EEF1A2, ATAD2, FOXP2, KIAA2022, WDR3, DNMT1, TMPO, CDK19, PDCD4, DMRTA1, MCM8, PLCB4, MCM7, PCGF3, HDRBS1, PARM1, SP100, LDB2, LEF1, MCM2, MCM3, MCM4, ECT2, MCM5, MCM6, CTSL, CTH, ZNF711, KPNA2, MELK, UBE2T, SPAST, FOXM1, KIAA0101, TCF7L2, TYMS, ZNF704, RGS12, HJURP, APEX1, GLRX, KAT2B, SP140L, RAD51AP1, CENPF, CENPE, CENPK, RACGAP1, TDP1, CENPU
CC:GO:0005829~cytosol	292	23.30407	2.36E-08	ALAD, S100A8, VPS54, AURKA, PTTG1, SYT7, GPCPD1, PRKG1, TPK1, PGPEP1, APP, SERPINE2, HOMER3, RBM8A, CH25H, SYK, BYSL, SKP2, WNK3, OPTN, NUDT11, CTNNA1, BCL2L11, NCAPD2, FARP2, PGM3, MAD2L1, SGO2, RCC2, ZWINT, CCR2, RGCC, KIF4A, ERBB4, NEK2, UBA5, CHEK1, CACNB3, CNTRL, EPHB3, EPHB4, TK1, GPD1L, VRK1, FBXO5, TCTN1, CDC42EP3, MOCS1, GPD1, SRP54, BHMT2, UAP1, KIF3A, SMAD9, NUF2, GGH, C16ORF89, TRIO, EPRS, CDC20, NDC80, SPDL1, SMAD2, KIF3C, DENND1B, NOTCH3, NOTCH1, CCT5, RGS2, KCNIP3, MTHFD2, CEP250, PIK3AP1, STX6, ZFP36, CDC6, RAP2A, ARHGEF2, EXOSC7, TPX2, TP53, CCT6A, ARHGEF9, FLNA, ATP6V1C2, RRM2, RRM1, FARSB, NUP107, SRGAP1, SERP1, RAP1GAP, ABHD5, ABI2, ZBTB16, APBB1IP, HMMR, STARD13, PLEKHG2, NCAPH, DAPP1, PLIN1, XBP1, SQSTM1, NCAPG, BCL2, BUB1, SULT1C2, ZWILCH, TBC1D1, PHLDA1, PLA2G16, NOS1, SPSB1, PDE3A, MID1, BIRC3, STAT3, CCNB1, CCNB2, CHML, KNL1, MT2A, AOX1, NINL, DPYD, PAICS, CALM1, DUSP6, ALDH1L1, GNPDA1, PRC1, XPO5, CEP78, ADH1C, SNRPD1, IQGAP3, PDE3B, ADH1B, DSTYK, IQGAP2, ADH1A, PNP, SLC7A5, KLHL2, EIF4EBP1, ASPA, ATAT1, NANS, ANK2, TIAM1, PDE4A, PDE4B, RGN, IL1B, SPR, STK39, MLKL, PRKACB, DNAJC3, SAR1B, RNF34, DNAJC1, C2CD2, CEP89, NCALD, STK26, FBP1, ACTN1, BICD1, DDIT4, TRIM37, SDCBP, AKAP7, STMN1, LRRK2, KALRN, FGFR1, EIF4E3, GNE, DIAPH3, CTPS1, RIOK1, RRAGD, CMPK1, OAZ3, ISYNA1, RHOBTB1, GALE, DOPEY2, NDRG2, GNMT, RHOBTB3, SEC61A2, CKAP5, RPGRIP1L, WIPI1, PDE7B, PLK4, PLCG1, FABP3, RAP1A, FABP4, PARD6G, FABP7, MYH10, KIF23, CDK19, NAMPT, KIF22, SEC24A, OGDHL, WWC1, PIP5K1B, NCS1, CAD, RHOU, PDCD4, PRMT3, KIF2C, PRMT1, SPRY1, PLCB4, MCM7, TRIM8, PAK3, SDPR, ACOT11, MGLL, PDE8B, CASP2, KHDRBS1, KIF14, CDK1, RSU1, KIF11, KIF15, PRKCH, NUP85, CDK6, ARHGAP29, ARHGAP24, ECT2, ARHGAP26, CTH, ATG4A, NUCB2, CA6, BUB1B, PDE9A, CA2, KPNA2, NUP160, HAUS1, SNX16, VIM, CYTH2, CYTH3, VARS, FAM13A, SEC62, TPM4, SEC63, ALDH1A1, TYMS, TFAM, TSC22D3, ATIC, INPP5J, PAFAH1B3, INPP5D, PIK3R3, HBB, GLRX, CENPO, RNF144B, CENPN, PDCD11, GMDS, CENPF, CENPE, CDC25C, CENPK, RACGAP1, EXO5, SMC2, CENPJ, CDC25B, SMC4, AMPD1, ITPA, CENPU

MF:GO:0005515~protein binding	674	53.790902	6.89E-09	PTGS2, LSM8, PPP2R5A, VPS54, TLDC1, RORC, SART3, NMRK1, TMEM140, B2M, PGR, OGN, APP, SERPINE2, INTS7, RAB27B, CCNA2, CDCA4, SYK, PTPRJ, LIFR, SKP2, CTNNA1, NME7, BCL2L11, NCAPD2, NPC1, SGO2, RCC2, MELTF, ZWINT, ZNF239, VGLL4, ORAI2, ODAM, ZNF614, KIF4A, ERBB4, CACNB2, GSTCD, UBA5, ZNF230, PRRC2B, CNTRL, MTIF3, NCAPG2, SYBU, PIP, NAT10, LAPTM4B, KIF3A, MKI67, ASXL1, ESRRG, NUF2, SPDL1, NDC80, KLF15, FAM131C, FNIP2, C16ORF87, RGS2, PKP2, TRPS1, SYTL4, PCNA, DEPTOR, SLC9A1, SEPHS1, EZH2, PLEKHG4B, SCRG1, HSF2, SERPINA5, SLC22A3, TRPV6, DPP4, SH3PXD2B, CDC7, STX6, CDC6, RAP2A, NFKBIZ, ARHGEF2, EXOSC7, TP53, TPX2, GTF2H3, ERLIN1, CCT6A, TTF2, FLNA, MYRIP, FANCD2, RRM2, PLXDC2, RRM1, G0S2, TXK, VCAN, CAND1, NUP107, THOC5, ARL4D, RASD1, SRGAP1, ARL4A, REPS2, ALDH18A1, C3, ABI2, C2ORF88, CCL28, APBB1IP, SF3B3, DAPP1, KIRREL, BUB1, WDR12, TBC1D1, TRIP13, MT1F, PHLDA1, SOAT1, FLRT3, CCNB1IP1, TRIM28, ZNF260, IGF1, ELAVL2, MID1, CCNB1, ZNF670, RASSF5, CCNB2, DUSP1, PLSCR4, TFRC, MT2A, ZBTB5, SECISBP2L, SH3RF2, USP49, DPYD, PHLDB2, SELE, BARD1, GNA14, GNPDA1, TSPAN1, PRC1, XPO5, STK36, SNRPD1, PDE3B, ADH1A, JAG1, LNX1, NRCAM, EIF4EBP1, ASPA, DAB2, ANK2, ZNF300, MDFIC, PDE4A, C8ORF4, IL15RA, PITPNC1, STK39, CTDSP2, DDX21, ELOVL6, DNAJC1, FLVCR1, RBFOX2, BPIFA2, ACTN4, NCALD, STK26, FBP1, ACTN1, TMSB10, JUNB, BICD1, WEE1, ZNF3, ZFP69B, TIMELESS, SMARCE1, HSPB8, SIX1, TFAP2B, TFAP2A, STMN1, LRRK2, SLC40A1, SMARCA4, CRACR2A, CCDC8, HMGB2, HMGB3, CYSLTR1, ADAMTSL3, NOSTRIN, CXXC5, IL33, TIMP2, MEIS1, ZNF330, OAZ3, TUBB, ISYNA1, MEIS2, POLE2, EGF, PLEKHS1, HELLS, GINS2, HERPUD1, HENMT1, GAREM1, NR4A2, SPPL2B, EFS, BRIP1, TEAD2, MUC7, FAM208B, FURIN, PLK4, TNFSF10, HDAC2, DNAJB9, FABP3, HDAC9, PMP2, MYH10, KIF23, ZKSCAN7, KIF22, E2F3, SEC24A, FIGNL1, E2F7, OGDHL, WWC1, PIP5K1B, GABBR1, PAWR, ZKSCAN3, RHOU, HTN3, SH2D4A, PRMT3, KIF2C, TSPAN12, SPRY1, CDC45, SLC1A2, PRMT1, HTN1, TMEM231, TRIM8, PAX9, HEY2, SNTB1, POLG2, CASP2, KDM5B, KIF14, CDK1, LIMK2, KIF15, NUSAP1, DIEXF, CDK6, NUP85, PBK, DHRS2, ADRB2, RFWD3, ADRB1, TBCB, SLC41A2, ATG4A, ERN1, PLLP, PDE9A, CA2, CPSF3, SEC23B, FKBP2, STON2, ABLIM1, HYLS1, VIM, HAUS1, NR3C2, NUP93, NFYB, NR3C1, NFYA, TSPYL4, VARS, TSPYL5, PLPP3, SEC63, APLP2, TSC22D1, TFAM, INPP5J, DNER, RNF128, SLC35B4, PAFAH1B3, INPP5D, HBB, SCNN1A, CHD4, EXO1, WDFY2, RNF144B, PDCD11, COL4A2, ADARB1, GMDS, SLC12A2, CEBPD, KLK3, CEBPG, ANXA1, FAM218A, CDC25C, SMC2, ADIPOQ, FBL, CDC25B, SMC4, CLPTM1, CCDC110, ZBED4, KDM4A, TBL1X, DMBT1, CTTNBP2NL, ATP1B1, HM13, S100A8, FAM20A, IL6ST, FAM20C, AQP5, AURKA, LPAR1, SYT7, PTTG1, PRKG1, ATP2B2, G2E3, ATP2B4, CD44, TRAK2, APOD, HOMER3, RBM8A, PLOD3, INSIG1, CREB3L1, H2AFY, ADGRB3, PRAME, POLH, BYSL, WNK3, CD40, DEPDC1, OPTN, RFC5, VEGFB, HES1, VEGFC, RFC3, UHRF1, NOP2, CD36, DCLRE1B, MAD2L1, RFC4, PIAS3, CNTROB, RGCC, RAB17, EFNA4, DBN1, FBXL2, FUS, LMNB1, NEK2, AKAP12, MME, CHEK1, EPHB4, TIPRL, TK1, VRK1, STX19, TCTEX1D2, SKA3, FBXO5, TMED10, AGRN, POLQ, WDHD1, OLFM2, TRAM1, HNRNPAB, NKRF, SRP54, SMAD9, NDFIP1, EPRS, TRIO, CDC20, SMAD2, TPD52L1, HOMER2, EPHA2, ABCG2, NOTCH3, NTRK3, NOTCH1, LAMA4, CCT5, CD55, CSRNP1, NIPSNAP1, HOPX, RAD54B, CRYM, ACVRL1, SLC15A2, CPEB3, CPEB4, KCNIP3, ZBTB38, FANCM, TNFRSF11A, AGPAT5, CEP250, FANCI, MCEE, GPX7, SMCO4, FAM129A, TOP2A, ZFYVE1, ZFP36, KCNMA1, CTBP2, LY96, NIP7, ICAM3, POLR1B, RAD51, EFHC2, SEMA4C, FARSB, SERP1, LCORL, RAP1GAP, STATH, ZBTB16, FAM46A, FAM46C, TPCN1, SEC14L1, STARD13, HMMR, NCAPH, NCAPG, SQSTM1, XBP1, BCL2, FAT1, ETV1, SULT1C2, ZWILCH, KIF21A, PLA2G16, NOS1, SPSB1, DLGAP5, FZD1, ILF3, AFF1, CDKN3, BIRC3, STAT3, MICALL1, C4ORF46, MEOX2, KNL1, FBLN5, KREMEN1, NINL, MEX3C, ATP6V0A4, APBB2, PAICS, CD14, TEX10, CALM1, KIF20A, CBX3, TLR3, FGF10, TTK, CBX1, FGF12, MCM10, KLHL2, KLHL7, ACSS1, TIAM1, GATA3, MLKL, PRKACB, RNF34, PAG1, RPL36AL, ARGLU1, DDX39A, SATB1, DTL, PLXNB1, CEP89, CST3, CST2, CST1, BASP1, NEBL, TRIM37, TNS1, CST5, DSP, SNRPA, SDCBP, AKAP7, RIPK4, ERC1, WNT5A, FGFR1, TSHZ2, BLM, MSMB, GNE, SOX4, MRAP2, GIPC2, RRAGD, RIOK1, DERL3, UBE2D4, ERO1A, ERO1B, ENTPD3, NDRG2, GNMT, MFAP3L, DEFB1, RNF13, RHOBTB3, SETDB1, TMEM97, CSTF3, TESC, CKAP5, RFX5, EEF1A2, RPGRIP1L, REEP5, FOXP2, TXNDC11, TRIM59, PLCG1, CD274, DNMT1, RAP1A, GLMN, WIF1, KCTD15, PARD6G, FAM84B, NAMPT, CEP57L1, MLPH, NCS1, LGR6, PDCD4, FAM83D, MCM8, PCGF3, MCM7, PLCB4, TMEM59, PAK3, SDPR, ATP8B1, SV2B, KHDRBS1, RSU1, SP100, MPP1, PEBP4, RUNX1T1, LDB2, LEF1, NRXN1, MCM2, ARHGAP24, MCM3, ECT2, MCM4, ARHGAP26, MCM5, MCM6, DAPK1, CTSL, CTH, NUCB2, ZNF711, BUB1B, SLPI, CTSC, KPNA2, SPAST, MELK, AOC3, SHCBP1, CKS1B, NUP160, PPP4R1, FOXM1, KIAA0101, CYTH2, CEP55, CYTH3, TCF7L2, MYOT, TPM4, HJURP, PIK3R3, APEX1, MYOC, CENPO, MSH6, GLRB, RAD51AP1, KAT2B, GIMAP7, CENPF, CENPE, SPARC, RACGAP1, CENPK, CENPJ, PRLR, TDP1, CKS2, CENPU, BMPR1B, IGFBP2, CSN3

MF:GO:0046872~metal ion binding	166	13.248204	0.0053304	GNA14, ALAD, PTGS2, PDE3B, MCM10, NMRK1, ATP2B2, ASPA, ATP2B4, ZNF300, PDE4A, PRIM2, PDE4B, CTDSP2, SAR1B, POLH, ZNF506, FBP1, ZNF8, NUDT11, OPTN, NME7, ZNF3, PGM3, ZFP82, ZFP69B, ZNF239, ZNF431, KALRN, ZNF614, TSHZ2, ME3, ADHFE1, ZNF77, GNE, AGFG2, NEK2, ENPP3, ENPP4, UBA5, ZNF230, RIOK1, AGMAT, TIMP2, ACAT1, ZNF618, ZNF330, PRUNE2, CASZ1, FBXO5, MOCS1, PLAG1, KLF7, ZNF529, LPO, SMAD9, HENMT1, ASXL1, SMYD3, BRIP1, SMAD2, KLF15, FURIN, FOXP2, RIMKLB, ITGA9, ZFHX4, TNFSF10, PDZD8, PDE7B, CADPS2, ATP2A3, TRPS1, HDAC9, PON3, ZKSCAN7, STEAP4, ACVRL1, MLPH, OGDHL, SOBP, CAD, ZKSCAN3, RHOU, HTN3, ZNF678, DMRTA1, ACVR1C, ZBTB38, PRMT3, PCGF3, TNFRSF11A, ZNF682, PAK3, MCEE, ZNF681, ZNF492, PDE8B, TRPV6, ZFYVE1, CDC7, KCNMA1, ZFP36, ARHGEF2, STS, ZNF280C, GEN1, NRXN3, PAPD7, RUNX1T1, TP53, PRKCH, GTF2H3, ADIPOR1, ARHGAP29, POLR1B, MCM2, NRXN1, TESMIN, NAALAD2, ZNF135, RRM2, ZNF711, PDE9A, CPSF3, YPEL1, ZNF558, ZNF556, CLCNKB, ZBTB16, ADAT1, COL9A1, ZNF704, COL27A1, BCL11A, ZNF850, MT1E, ETFDH, GALNT15, GALNT16, APEX1, GALNT13, MYOC, MT1F, EXO1, WDFY2, ADARB1, ZNF260, ZFP1, ZNF667, DGKH, PDE3A, RACGAP1, EXO5, AMPD1, ZNF670, RASSF5, ITPA, PRLR, ZBED4, MT2A, AOX1, ZBTB5, NLN, DPYD, BMPR1B
MF:GO:0005524~ATP binding	147	11.731844	7.64E-07	MOK, ATP1B1, STK36, FAM20C, DSTYK, TTK, AURKA, PRKG1, NMRK1, TPK1, ATP2B2, ACSS1, ATP2B4, STK39, DDX21, MLKL, PRKACB, SYK, DDX39A, STK26, UBE2J1, WNK3, WEE1, NME7, C10ORF2, RFC5, RFC4, RIPK4, LRRK2, KALRN, SMARCA4, ABCA8, FGFR1, KIF4A, ABCA9, BLM, ERBB4, DNAH14, GNE, NEK2, STK17B, CTPS1, UBA5, CHEK1, RIOK1, EPHB3, EPHB4, ABCA6, CMPK1, TK1, UBE2D4, VRK1, NAT10, ENTPD3, POLQ, HELLS, RHOBTB3, KIF3A, MKI67, TRIO, EPRS, BRIP1, ATAD2, KIF3C, ABCB6, EPHA2, ABCG2, RIMKLB, NTRK3, PLK4, CCT5, ATP2A3, RAD54B, DDX52, MYH10, ATAD2B, CDK19, KIF23, KIF22, SEPHS1, ACVRL1, FIGNL1, TTLL4, PIP5K1B, CAD, TTLL7, TTLL1, ACVR1C, FANCM, KIF2C, MCM8, MCM7, PAK3, ATP8B1, TOP2A, KIF14, CDC7, CDK1, CDC6, KIF11, LIMK2, KIF15, TP53, TPX2, PRKCH, PKDCC, CDK6, CCT6A, PBK, MCM2, MCM3, MCM4, TTF2, MCM5, DAPK1, RAD51, MCM6, MAST4, RRM1, ERN1, FARSB, BUB1B, NRK, TXK, UBE2S, MELK, UBE2T, SPAST, ALDH18A1, VARS, ACSL1, FIGN, CKMT2, BUB1, KIF21A, CHD4, ABCA13, TRIP13, MSH6, PDK4, DGKH, CENPE, SMC2, SMC4, BMPR1B, PAICS, KIF20A

Table 2: KEGG analysis of DEGs in SACC samples.

Term	Count	%	Pvalue	Genes
hsa05200:Pathways cancer	43	3.4317638	0.0214456	WNT5A, CKS1B, FGFR1, E2F3, PTGS2, LPAR3, FGF10, FGF12, ZBTB16, LPAR1, CXCL12, TCF7L2, PLCB4, BCL2, PRKACB, EGF, PIK3R3, LAMB1, MSH6, COL4A2, PTGER3, CTBP2, KLK3, TP53, RUNX1T1, FZD1, SKP2, IGF1, LEF1, CDK6, SMAD2, CTNNA1, BIRC3, STAT3, DAPK1, RAD51, VEGFB, VEGFC, RASSF5, LAMA4, HDAC2, PLCG1, CKS2
hsa04110:Cell cycle	31	2.4740623	1.32E-08	E2F3, DBF4, TTK, CHEK1, PTTG1, CDC45, MCM7, BUB1, CCNA2, CDC7, CDC6, CDK1, TP53, SKP2, SMAD2, CDK6, CDC20, MCM2, CDC25C, MCM3, MCM4, WEE1, MCM5, CDC25B, MCM6, CCNB1, MAD2L1, HDAC2, CCNB2, PCNA, BUB1B
hsa04970:Salivary secretion	27	2.1548284	7.46E-10	ATP1B1, STATH, AQP5, PRKG1, HTN3, ATP2B2, HTN1, PLCB4, ATP2B4, TRPV6, PRKACB, KCNMA1, LPO, NOS1, SLC12A2, CST3, LYZ, CST2, MUC7, CST1, ADRB2, ADRB1, CST5, ADRA1A, SLC9A1, CALM1, DMBT1
hsa04141:Protein processing in endoplasmic reticulum	23	1.8355946	0.0117043	HERPUD1, TUSC3, SEC24A, RRBP1, UBE2J1, MAN1A1, SEC62, DERL3, SEC63, UBE2D4, ERO1A, ERO1B, XBP1, BCL2, ERN1, DNAJC3, SAR1B, SR4, TRAM1, DNAJC1, SEC23B, SEC61A2, SSR3
hsa04114:Oocyte meiosis	17	1.3567438	0.0118721	CDK1, CPEB3, PPP2R5A, CPEB4, IGF1, AURKA, CDC20, PTTG1, CDC25C, PGR, CCNB1, CCNB2, MAD2L1, BUB1, FBXO5, PRKACB, CALM1
hsa04914:Progesterone -mediated oocyte maturation	15	1.1971269	0.0070197	CDK1, CPEB3, CPEB4, PDE3B, IGF1, CDC25C, CDC25B, CCNB1, PGR, CCNB2, MAD2L1, BUB1, PRKACB, PIK3R3, CCNA2
hsa00240:Pyrimidine metabolism	14	1.1173184	0.0496292	CTPS1, CAD, POLR1B, PNP, NME7, CMPK1, TK1, TYMS, POLE2, RRM2, RRM1, PRIM2, ENTPD3, DPYD
hsa04923:Regulation of lipolysis in adipocytes	13	1.03751	0.001048	PLA2G16, PTGER3, PTGS2, ABHD5, PDE3B, PRKG1, ADRB2, ADRB1, PLIN1, FABP4, MGLL, PRKACB, PIK3R3
hsa05222:Small cell	13	1.03751	0.031455	CKS1B, COL4A2, E2F3, PTGS2, SKP2, TP53, CDK6, BIRC3, LAMA4, BCL2, CKS2, LAMB1, PIK3R3
hsa03030:DNA replication	12	0.9577015	5.87E-05	RFC5, RFC3, RFC4, MCM7, POLE2, PRIM2, PCNA, MCM2, MCM3, MCM4, MCM5, MCM6
hsa03060:Protein export	7	0.5586592	0.0070437	SRP54, SEC11C, SPCS3, SRPRB, SEC62, SEC63, SEC61A2
hsa03430:Mismatch repair	6	0.4788508	0.0294943	EXO1, RFC5, MSH6, RFC3, RFC4, PCNA

GO and KEGG analysis of DEGs

To analyze the enrichment information and biological process of DEGs, functional and pathway analyses were applied using DAVID. The BP, CC and MF was required for GO analysis. The significant module of BP, CC and MF contained 136, 55 and 40 terms under P value ≤ 0.01, separately. As Table 1 showed, the maximum of BP module included 94 DEGs (7.5%). The maximum of CC module was cytoplasm included 427 DEGs (34.1%). The maximum of MF module included 674 DEGs (53.8%). The three most BP module comprised signal transduction (GO: 0007165), cell division (GO: 0051301) and negative regulation of transcription from RNA polymerase II promoter (GO: 0000122). The three most CC module enriched cytoplasm (GO: 0005737), nucleus (GO: 0005634) and cytosol (GO: 0005829). The three most MF module contained protein binding (GO: 0005515), metal ion binding (GO: 0046872) and ATP binding (GO: 0005524). The change of KEGG was mainly enriched in pathways in cancer (hsa05200), cell cycle (hsa04110) and salivary secretion (hsa04970).

Table 3: Functional roles of 18 candidate gene.

No.	Gene symbol	Full name	Function
1	DLGAP5	DLG Associated Protein 5	Potential cell cycle regulator that may play a role in carcinogenesis of cancer cells. Mitotic phosphoprotein regulated by the ubiquitin-proteasome pathway.
2	KIF11	Kinesin Family Member 11	This gene encodes a motor protein that belongs to the kinesin-like protein family. The function of this gene product includes chromosome positioning, centrosome separation and establishing a bipolar spindle during cell mitosis.
3	CCNB2	Cyclin B2	Diseases associated with CCNB2 include Breast Cancer. Among its related pathways are GPCR Pathway and Cell cycle Role of APC in cell cycle regulation.
4	BUB1	BUB1 Mitotic Checkpoint Serine/ Threonine Kinase	Mutations in this gene have been associated with aneuploidy and several forms of cancer. Diseases associated with BUB1 include Mosaic Variegated Aneuploidy Syndrome and Colorectal Cancer.
5	ZWINT	ZW10 Interacting Kinetochore Protein	The encoded protein localizes to prophase kinetochores before ZW10 does and it remains detectable on the kinetochore until late anaphase. Alternatively spliced transcript variants encoding different isoforms have been found for this gene.
6	NUP160	Nucleoporin 160	NUP160 is 1 of up to 60 proteins that make up the 120-MD nuclear pore complex, which mediates nucleoplasmic transport. Among its related pathways are Transport of the SLBP independent Mature mRNA and Metabolism of proteins.
7	CENPF	Centromere Protein F	The localization of this protein suggests that it may play a role in chromosome segregation during mitotis. Autoantibodies against this protein have been found in patients with cancer or graft versus host disease.
8	TOP2A	DNA Topoisomerase II Alpha	The gene encoding this enzyme functions as the target for several anticancer agents and a variety of mutations in this gene have been associated with the development of drug resistance. Reduced activity of this enzyme may also play a role in ataxia-telangiectasia.
9	PPP2R5A	Protein Phosphatase 2 Regulatory Subunit B'Alpha	Protein phosphatase 2A is one of the four major Ser/Thr phosphatases, and it is implicated in the negative control of cell growth and division. It consists of a common heteromeric core enzyme, which is composed of a catalytic subunit and a constant regulatory subunit that associates with a variety of regulatory subunits.
10	KIF2C	Kinesin Family Member 2C	This gene encodes a kinesin-like protein that functions as a microtubule-dependent molecular motor. The encoded protein can depolymerize microtubules at the plus end, thereby promoting mitotic chromosome segregation.
11	CCNB1	Cyclin B1	The protein encoded by this gene is a regulatory protein involved in mitosis. Among its related pathways are GPCR Pathway and Cell cycle Role of APC in cell cycle regulation.
12	KIF23	Kinesin Family Member 23	This protein has been shown to cross-bridge antiparallel microtubules and drive microtubule movement in vitro. Alternate splicing of this gene results in multiple transcript variants.
13	CDK1	Cyclin Dependent Kinase 1	Mitotic cyclins stably associate with this protein and function as regulatory subunits. Alternatively spliced transcript variants encoding different isoforms have been found for this gene.
14	RRM2	Ribonucleotide Reductase Regulatory Subunit M2	Synthesis of the encoded protein (M2) is regulated in a cell-cycle dependent fashion. Transcription from this gene can initiate from alternative promoters, which results in two isoforms that differ in the lengths of their N-termini.
15	BUB1B	BUB1 Mitotic Checkpoint Serine/ Threonine Kinase B	The protein has been localized to the kinetochore and plays a role in the inhibition of the anaphase-promoting complex/cyclosome (APC/C), delaying the onset of anaphase and ensuring proper chromosome segregation. Impaired spindle checkpoint function has been found in many forms of cancer.
16	NDC80	NDC80, Kinetochore Complex Component	This protein functions to organize and stabilize microtubule-kinetochore interactions and is required for proper chromosome segregation.
17	TPX2	TPX2, Microtubule Nucleation Factor	Spindle assembly factor required for normal assembly of mitotic spindles. At the onset of mitosis, GOLGA2 interacts with importin-alpha, liberating TPX2 from importin-alpha, allowing TPX2 to activates AURKA kinase and stimulates local microtubule nucleation
18	CKAP5	Cytoskeleton Associated Protein 5	This protein has two distinct roles in spindle formation; it protects kinetochore microtubules from depolymerization and plays an essential role in centrosomal microtubule assembly. It also plays a role in translation of the myelin basic protein (MBP) mRNA by interacting with heterogeneous nuclear ribonucleoprotein (hnRNP) A2, which associates with MBP. Alternatively spliced transcript variants encoding different isoforms have been identified.

The results of KEGG analysis was shown in Table 2.

The network construction of DEGs

In an attempt to understand the network of DEGs, the interaction network of 1282 genes was constructed using STRING and Cytoscape. The most significant section with a total of 47 hub genes was shown with MCODE (Figure 1B), including NCAPG, DLGAP5, KIF15, MELK, CCNA2, CENPO, CENPU, KIF11, ASPM, TTK, CCNB2, CENPK, KIF4A, CASC5, BUB1, RCC2, AURKA, SGOL2, NUF2, PBK, NEK2, MAD2L1, SPDL1, ZWINT, NUP160, CENPF, TOP2A, CEP55, KIF20A, CENPN, CDC20, CENPE, PPP2R5A, KIF2C, CCNB1, KIF23, CDK1, ZWILCH, NUSAP1, RRM2, NUP85, NUP107, BUB1B, PRC1, NDC80, TPX2 and CKAP5.

Enrichment and analysis of candidate genes from hub genes

Following the information of 47 hub genes, a total of 18 candidate genes were applied using salivary gland adenoid cystic carcinoma dataset of Oncomine, consisting of 3 down regulated genes and 15 up regulated genes between salivary gland and salivary gland adenoid cystic carcinoma (Figure 2). Table 3 presents the names, abbreviations and functions for these candidate genes.

Pharmaceutical target analysis of candidate genes

To observe the pharmaceutical target of candidate genes, network of target and interaction network were performed using cBio Portal online analysis in the final part of the research. The drug information of 18 candidate genes were analyzed with 10% filter configuration as mentioned in Methods (Figure 3). It was found that drugs of specified genes were focused on TOP2A, KIF11 and RRM2.

Discussion

Salivary gland adenoid cystic carcinoma, a type of ACC arising from salivary gland, is a malignance that causes substantial mortality with malignant growth and metastasis [2,17,18]. These aggressive characters of this carcinoma account for the initiation and progression

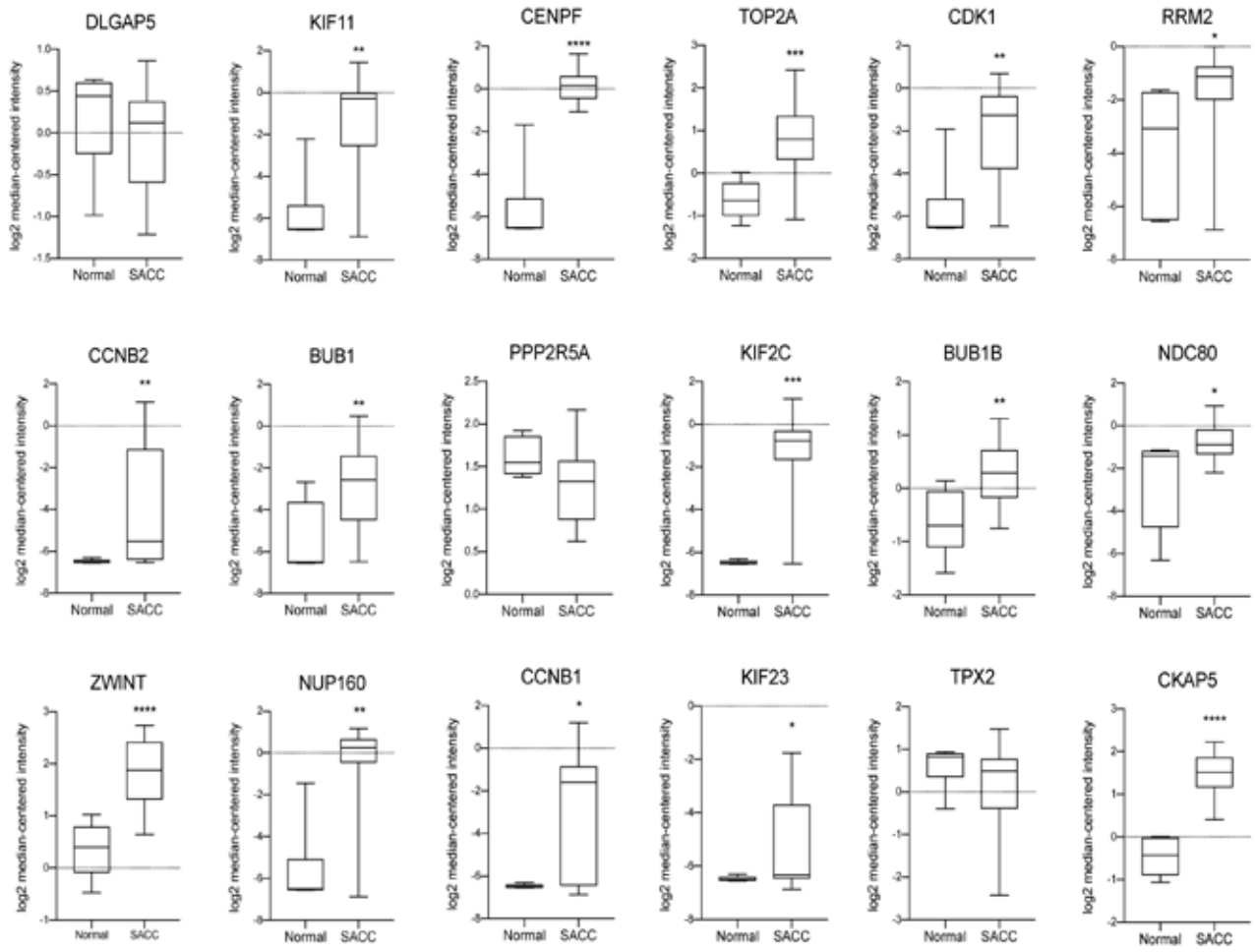

Figure 2: Oncomine analysis of 18 candidate genes. The expression profile of 1282 genes was performed using Oncomine online analysis between SACC *vs.* normal tissue.

of SACC. The SACC patients are in need of effective therapeutic strategy with drug research and development [19]. SACC cases are not candidates for curative treatment with pharmaceutical products. Thus, potential biomarkers for treatment with high efficiency are strongly demanded. In this study, the significant DEGs from 2 GEO datasets were investigated after bioinformatic analysis in order to research and develop drugs.

In the current study, it was presented that 1282 DEGs were overlapped using GEO2R analysis from 2 microarray datasets. These 2 SACC datasets contained a total of 15979 DEGs between normal human salivary gland and SACC samples. There would be more indication for further research to investigate the biological function and pathway which 1282 DEGs involved in. As mentioned in Table 1, these DEGs were mainly enriched in signal transduction, cell division and negative regulation of transcription from RNA polymerase II promoter. It is now well established from a variety of studies that signal transduction and cell division play significant roles in carcinogenesis of tumors [20-22]. It is somewhat surprising that the third most DEGs (4.948%) are involved in the negative regulation of transcription from RNA polymerase II promoter. RNA polymerase II is one of the three RNA polymerase enzymes found in the nucleus [23,24]. It catalyzes the transcription of DNA to synthesize precursors of mRNA and most non-coding RNA. Previous research has established that RNA polymerase II-associated factor can combine with other subunits in order to form one complex, which enables various functions, including cell cycle regulation and mRNA quality control [25,26]. It is thus suggested that pharmaceutical research should be directly aimed at the biological precession of regulation of transcription from RNA polymerase II promoter.

According to the GO analysis, cell component of DEGs were enriched in cytoplasm (34%) and nucleus (33%), respectively. However, P value was different between these two cell components. P value of cytoplasm was 3.85×10.8, whereas P value of nucleus was only 0.029. A possible explanation for this might be that it is required to conduct more research to elaborate the different expression profile of SACC with *in vivo* and *in vitro* experiment.

After STRING and DAVID analysis, 18 candidate genes were determined from analysis of Oncomine. Oncomine analysis of SACC *vs.* normal tissue was applied for verifying the most significant DEGs. Subsequently, the drug target of candidate genes was performed using cBio Portal online analysis. As shown in Table 2, there are three most relevant target molecular including TOP2, KIF11, CDK1, RRM2 and KIF2C. The total of 25 TOP2 drug contained 15 drugs approved by Food and Drug Administration (FDA). The all 4 drugs of RRM2 were exhibited as FDA approved drugs. The other 3 candidate genes had all drugs without approval by FDA. There was still even no drug acted with the rest candidate genes, indicating that putative drug can be

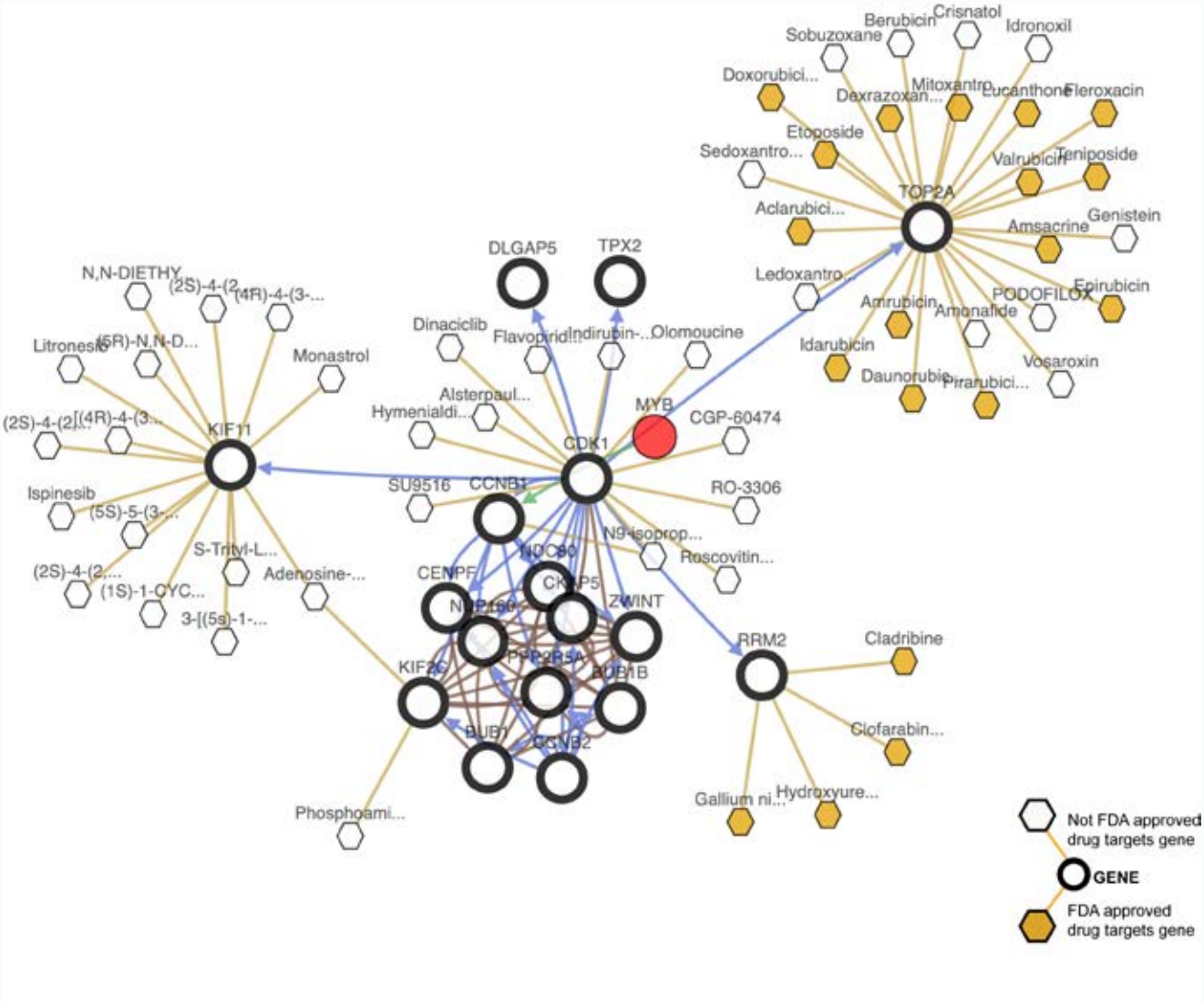

Figure 3: Interaction network analysis of 18 candidate genes. Nodes with bold black outline represent candidate genes.

drawn from pharmaceutical research of these gene in the future study.

Acknowledgment

The authors thank GEO for providing data.

References

1. Goulart-Filho JAV, Montalli VAM, Passador-Santos F, de Araújo NS, de Araújo VC. Role of apoptotic, autophagic and senescence pathways in minor salivary gland adenoid cystic carcinoma. Diagn Pathol. 2019;14(1):14.

2. Megwalu UC, Sirjani D. Risk of Nodal Metastasis in Major Salivary Gland Adenoid Cystic Carcinoma. Otolaryngol Head Neck Surg. 2017;156(4):660-4.

3. Yoshimoto M, Tokuda A, Nishiwaki K, Sengoku K, Yaginuma Y. Abnormal Expression of PICT-1 and Its Codon 389 Polymorphism Is a Risk Factor for Human Endometrial Cancer. Oncology. 2018;95(1):43-51.

4. Zhang X, Pan Y, Fu H, Zhang J. Nucleolar and Spindle Associated Protein 1 (NUSAP1) Inhibits Cell Proliferation and Enhances Susceptibility to Epirubicin In Invasive Breast Cancer Cells by Regulating Cyclin D Kinase (CDK1) and DLGAP5 Expression. Med Sci Monit. 2018;24:8553-64.

5. Daoud M, Mayo M. A survey of neural network-based cancer prediction models from microarray data. Artif Intell Med. 2019;97:204-14.

6. Yin F, Yi S, Wei L, Zhao B, Li J, Cai X, et al. Microarray-based identification of genes associated with prognosis and drug resistance in ovarian cancer. J Cell Biochem. 2019;120(4):6057-70.

7. Edgar R, Domrachev M, Lash AE. Gene Expression Omnibus: NCBI gene expression and hybridization array data repository. Nucleic Acids Res. 2002;30(1):207-10.

8. Andersson MK, Afshari MK, Andren Y, Wick MJ, Stenman G. Targeting the Oncogenic Transcriptional Regulator MYB in Adenoid Cystic Carcinoma by Inhibition of IGF1R/AKT Signaling. J Natl Cancer Inst. 2017;109(9).

9. Huang DW, Sherman BT, Tan Q, Collins JR, Alvord WG, Roayaei J, et al. The DAVID Gene Functional Classification Tool: a novel biological module-centric algorithm to functionally analyze large gene lists. Genome Biol. 2007;8(9):R183.

10. Al-Mubaid H. Gene multifunctionality scoring using gene ontology. J Bioinform Comput Biol. 2018;16(5):1840018.

11. Tanabe M, Kanehisa M. Using the KEGG database resource. Curr Protoc Bioinformatics. 2012;Chapter 1: Unit1.12.

12. Szklarczyk D, Gable AL, Lyon D, Junge A, Wyder S, Huerta-Cepas J, et al. STRING v11: protein-protein association networks with increased coverage, supporting functional discovery in genome-wide experimental datasets. Nucleic Acids Res. 2019;47(D1):D607-13.

13. Bandettini WP, Kellman P, Mancini C, Booker OJ, Vasu S, Leung SW, et al. MultiContrast Delayed Enhancement (MCODE) improves detection of subendocardial myocardial infarction by late gadolinium enhancement cardiovascular magnetic resonance: a clinical validation study. J Cardiovasc Magn Reson. 2012;14:83.

14. Rhodes DR, Kalyana-Sundaram S, Mahavisno V, Varambally R, Yu J, Briggs BB, et al. Oncomine 3.0: genes, pathways, and networks in a collection of 18,000 cancer gene expression profiles. Neoplasia. 2007;9(2):166-80.

15. Frierson HF Jr, El-Naggar AK, Welsh JB, Sapinoso LM, Su AI, Cheng J, et al. Large scale molecular analysis identifies genes with altered expression in salivary adenoid cystic carcinoma. Am J Pathol. 2002;161(4):1315-23.

16. Gao J, Aksoy BA, Dogrusoz U, Dresdner G, Gross B, Sumer SO, et al. Integrative analysis of complex cancer genomics and clinical profiles using the cBioPortal. Sci Signal. 2013;6(269):pl1.

17. Demirci H, Vine AK, Elner VM. Choroidal metastasis from submandibular salivary gland adenoid cystic carcinoma. Ophthalmic Surg Lasers Imaging. 2008;39(1):57-9.

18. Portilla Blanco RR, Roberts Martinez-Aguirre I, Ponton Mendez P, Zarzosa Martin ME, Perez-Salvador Garcia E. Choroidal metastasis of a minor salivary gland adenoid cystic carcinoma: A case report. Arch Soc Esp Oftalmol. 2018;93(7):360-4.

19. Chen C, Choudhury S, Wangsa D, Lescott CJ, Wilkins DJ, Sripadhan P, et al. A multiplex preclinical model for adenoid cystic carcinoma of the salivary gland identifies regorafenib as a potential therapeutic drug. Sci Rep. 2017;7(1):11410.

20. Gu HZ, Lin RR, Wang HC, Zhu XJ, Hu Y, Zheng FY. Effect of Momordica charantia protein on proliferation, apoptosis and the AKT signal transduction pathway in the human endometrial carcinoma Ishikawa H cell line *in vitro*. Oncol Lett. 2017;13(5):3032-8.

21. Naher L, Kiyoshima T, Kobayashi I, Wada H, Nagata K, Fujiwara H, et al. STAT3 signal transduction through interleukin-22 in oral squamous cell carcinoma. Int J Oncol. 2012;41(5):1577-86.

22. Yin Y, Dou X, Duan S, Zhang L, Xu Q, Li H, et al. Downregulation of cell division cycle 25 homolog C reduces the radiosensitivity and proliferation activity of esophageal squamous cell carcinoma. Gene. 2016;590(2):244-9.

23. Hochberg-Laufer H, Shav-Tal Y. Active RNA polymerase II curbs chromatin movement. J Cell Biol. 2019;218(5):1427-8.

24. Price DH. Transient pausing by RNA polymerase II. Proc Natl Acad Sci U S A. 2018;115(19):4810-2.

25. Joo YJ, Ficarro SB, Marto JA, Buratowski S. *In vitro* assembly and proteomic analysis of RNA polymerase II complexes. Methods. 2019;159-160:96-104.

26. Petrenko N, Jin Y, Dong L, Wong KH, Struhl K. Requirements for RNA polymerase II preinitiation complex formation *in vivo*. Elife. 2019;8.